STRIPLINE ANTENNA WITH ELLIPTICAL DIPOLES - THEORETICAL AND EXPERIMENTAL CONSIDERATIONS

Gheorghe MORARIU*, Ecaterina-Liliana MIRON, Mihai MACHEDON-PISU*, Cristina MOŞNEAGU*, Andreea MOCANU***

*"Transilvania" University of Brasov, **"Henri Coandă" Air Force Academy, Braşov, Romania

Abstract*: The paper presents the main theoretical and practical aspects regarding stripline antenna with elliptical dipoles. There are presented design principles of the stripline antenna, their shape and physical dimensions. The material outlines specific characteristics of the stripline antenna with elliptical dipoles. The characteristics are investigated experimentally.*

Keywords*: stripline antenna, elliptical dipole, microstrip, microwave circuit.*

1. INTRODUCTION

At the same time increasing importance of wireless communication systems and personnel IT (information technologies) services (e.g., Bluetooth) increasing efforts are devoted to the design and implementation of novel microstrip structures from miniaturized electronic circuits to the antenna arrays. One major application is design of microstrip antennas which are attractive candidates for adaptive systems in the present and future communication systems. Their main advantages are light weight, low cost, planar or conformal layout, good gain (the gain obtained are comparable with gain of big classical antennas), and ability of integration with electronic or signal processing circuitry (Wong, 1999).

On the other hand, designing active/passive microwave circuits requires understanding of both mathematical relations (i.e., the theory) and applications (i.e., computer simulations as well as measurements).

Mathematical relations exist for only simple, idealized microstrip structures and may help to understand only the fundamentals.

This article describes the design, architecture and testing of stripline antenna with elliptical dipoles.

2. THE STRIPLINE ANTENNA WITH ELLIPTICAL DIPOLES

2.1 Design Principles. The resonant frequency selected for the design is 900 MHz. Theoretical and real wavelength is (Balanis, 1997):

$$f = 900\text{MHz} \Rightarrow$$

$$\Rightarrow \lambda_{th} = \frac{c}{f} = \frac{3\cdot 10^8}{9\cdot 10^8} = 33\,\text{cm} \qquad (1)$$

$$\lambda_{real} = \frac{\lambda_{th}}{\sqrt{\varepsilon_r}} = \frac{33}{1.61} = 20.5\text{cm} \qquad (2)$$

Here, c and ε_r are speed of light and effective relative permittivity.

The dimensions of the elliptical radiant element (a, b – half of the ellipse axis) are:

$$2a = \frac{\lambda_{th}}{4} \Rightarrow a = \frac{\lambda_{th}}{8} = 4.125\text{cm} \qquad (3)$$

$$\frac{a+b}{a} = \frac{a}{b} \Rightarrow b = 0.61\cdot 4.125 = 2.51\text{cm} \quad (4)$$

(according to optimal interpolation ratio – *golden cut* of the ellipse).

The size of the ellipse was calculated using λ_{th}, and to calculate the size of the slot type resonator was used λ_{real}.

For the calculus of the ellipse axis intersections, in case of higher harmonics, it was used the interpolation method (Morariu, 2009; Evangelos, 2006:294-297) on the cylindrical resonator by approximation at the elliptical boundaries (figure 1 and figure 2).

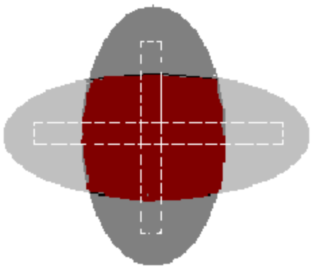

Fig. 1 Physical resonant cavity

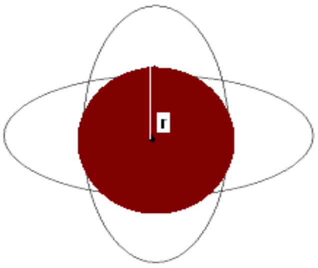

Fig. 2 Equivalent cavity used for calculation

The method consist in the equivalence of common radiating surfaces to those two stripline dipoles superimposed and separated by the dielectric layer as in figure 1, with an equivalent circular area presented in figure 2, neglecting the transfer radiation on the elliptical boundary and dipole plane behind the dielectric (their influence is minimal).

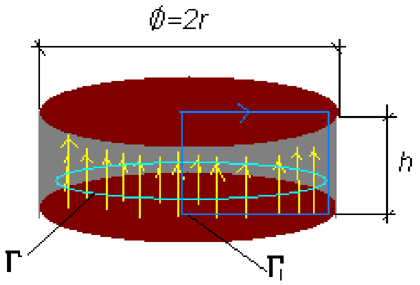

Fig. 3 Stripline equivalent resonator

Applying this procedure it is obtain a stripline cylindrical resonant cavity like in Figure 3, whose resonance frequency is derived using the calculation for the variation of high frequency electromagnetic field between plates of the parallel circular plane capacitor with dielectric ε_r.

Calculation of components B and E of the radiating electromagnetic field is obtained by applying the integral form of Maxwell equations iteratively as follows.

- Equivalent stripline cylindrical resonant cavity

$$\oint F \cdot dl = \iint_{\Sigma} \nabla \times F \cdot ds \qquad (5)$$

$$c^2 \nabla \times B = \frac{\partial}{\partial t} E \qquad (6)$$

$$\nabla \times E = -\frac{\partial}{\partial t} B \qquad (7)$$

$$\oint_{\Gamma_1} E \cdot dl = -\frac{\partial}{\partial t} \iint_{\Sigma_1} B \qquad (8)$$

$$c^2 \oint_{\Gamma} B \cdot dl = \frac{\partial}{\partial t} \iint_{\Sigma} E \cdot ds \qquad (9)$$

$$E = E_0 \cdot e^{j\omega t} \qquad (10)$$

$$c^2 B \cdot 2\pi \cdot r = \frac{\partial}{\partial t} \iint E_0 \cdot e^{j\omega t} \qquad (11)$$

$$c^2 B \cdot 2\pi \cdot r = \frac{\partial}{\partial t} E_0 \cdot e^{j\omega t} \int_0^r 2\pi \cdot r \cdot dr \qquad (12)$$

$$c^2 B \cdot 2\pi \cdot r = E_0 \cdot j\omega \cdot e^{j\omega t} \cdot \pi \cdot r^2 \qquad (13)$$

$$\Rightarrow B_1 = \frac{j\omega \cdot r}{2c^2} \cdot E_0 \cdot e^{j\omega t} \qquad (14)$$

which is the first field iteration.

$$\oint_{\Gamma} E \cdot dl = -\frac{\partial}{\partial t} \iint_{\Sigma_{\Gamma 1}} B_1 \cdot ds \qquad (15)$$

$$-h \cdot E_1 = -\frac{\partial}{\partial t} \int_0^r \frac{j\omega \cdot r}{2c^2} \cdot E_0 \cdot e^{j\omega t} \cdot ds \qquad (16)$$

$$-h \cdot E_1 = \frac{\omega^2 \cdot E_0 \cdot e^{j\omega t}}{2c^2} \int_0^r r \cdot dr \cdot h \qquad (17)$$

where $ds = dr \cdot h$ (18)

$$-E_1 = \frac{\omega^2 r^2 E_0}{4c^2} \cdot e^{j\omega t} \qquad (19)$$

$$\Rightarrow E_1 = -\frac{\omega^2 r^2 E_0}{2c^2} \cdot e^{j\omega t} \qquad (20)$$

$$E_T = E + E_1 \qquad (21)$$

For the second iteration:

$$c^2 \oint B_2 \cdot dl = \frac{\partial}{\partial t} \iint E_1 \cdot ds \qquad (22)$$

$$c^2 \cdot 2\pi \cdot r \cdot B_2 = \frac{\partial}{\partial t}\iint -\frac{\omega^2 r^2 E_0}{4c^2}\cdot e^{j\omega t}\cdot ds \quad (23)$$

where: $ds = 2\pi r \cdot dr$ (24)

$$B_2 = \frac{-1}{2\pi \cdot r \cdot c^2}\frac{\partial}{\partial t}\int_0^r 2\pi r \frac{\omega^2 r^2}{2^2 c^2} E_0 e^{j\omega t} dr \quad (25)$$

$$\oint E_2 \cdot dl = -\frac{\partial}{\partial t}\int_0^r B_2 \cdot h \cdot dr \quad (26)$$

$$-E_2 \cdot h = -\frac{\partial}{\partial t} h \int_0^r B_2 \cdot dr \quad (27)$$

$$\Rightarrow E_2 = -\frac{\partial}{\partial t}\int_0^r \frac{j\omega^3 r^3}{2^4 c^4}\cdot E_0 \cdot e^{j\omega t}\cdot dr \quad (28)$$

$$E = E + E_1 + E_2 + \ldots\ldots \quad (29)$$

$$E_T = E\left[1 - \frac{(\omega r)^2}{(2c)^2} + \frac{(\omega r)^4}{(2c)^4}\frac{1}{2^2} - \frac{(\omega r)^6}{(2c)^6}\frac{1}{6^2} + \ldots\right] \quad (30)$$

$$E_T = E\left[1 - \left(\frac{\omega \cdot r}{2c}\right)^2 \cdot \frac{1}{(1!)^2} + \left(\frac{\omega \cdot r}{2c}\right)^4 \frac{1}{(2!)^2} - \left(\frac{\omega \cdot r}{2c}\right)^6 \cdot \frac{1}{(3!)^2} + \ldots\right] \quad (31)$$

Naming: $x = \frac{\omega}{c} r$ (32)

$$E_T = E\left(1 - \frac{1}{1^2}\left(\frac{x}{2}\right)^2 + \frac{1}{(1\cdot 2)^2}\left(\frac{x}{2}\right)^4 - \frac{1}{(1\cdot 2\cdot 3)^2}\left(\frac{x}{2}\right)^6 + \ldots\right) \quad (33)$$

$$E_T = E \cdot J_1 \quad (34)$$

Bessel function $J_1(x)$ shall be cancelled for x = 2.41; 5.52; 8.2.

- For the equivalent cylindrical resonant cavity:

$r = b = 2.51\text{cm} = 2.51 \cdot 10^{-2}\,\text{m}$

The first resonance frequency (x = 2.41) is:

$$v = \frac{c}{\sqrt{\varepsilon_r}} \Rightarrow f = \frac{c \cdot x}{2\pi r \sqrt{\varepsilon_r}} = 2.85\text{GHz} \quad (35)$$

(the dielectric permittivity is $\varepsilon_r = 2.6$)

The second resonance frequency (x = 5.52) is f = 6.52GHz.

- Planar resonant cavity (Marchais, 2006: 319-322)

It is positioned symmetrically on the major axis of the ellipse, having the form and dimensions presented in figure 4.

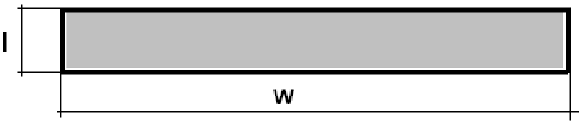

Fig. 4 Stripline resonant cavity

According to (2) the dimensions are:

$l = 0.52\text{cm} = 0.52 \cdot 10^{-2}\,\text{m}$

$w = 5.125\text{cm} = 5.125 \cdot 10^{-2}\,\text{m}$

Resonance modes are E_{m0n}.

$$\lambda_{rez} = \frac{2 \cdot \sqrt{\varepsilon_r}}{\sqrt{\left(\frac{m}{l}\right)^2 + \left(\frac{n}{w}\right)^2}} \quad (36)$$

$$f_{rez} = \frac{c}{\lambda_{rez}\sqrt{\varepsilon_r}} \quad (37)$$

E_{001} mode implies m = 0, w = 5.125cm, n = 1; according to (36), for $\varepsilon_r = 2.6$, the resonance wavelength is $\lambda_{rez} = 16.5$cm, and the resonance frequency is $f_{rez} = 1.13$GHz.

In case of open dipole antenna configuration (λ/2) with elliptical radiating elements and slot resonators, oscillating process take place and for slot length w = λ/4. This property lowers minimum operating frequency of the antenna at:

$$f_o = \frac{f_{rez}}{4} = 282.5\text{MHz} \quad (38)$$

According to (36), (37), (38), E_{00n} resonance modes determines resonance frequencies (n > 1) in the antenna $f = nf_o$, widening emission/reception spectrum of the antenna.

E_{101} mode leading to higher resonance frequencies, which in accordance with relations (36) and (37) starting with 11GHz.

- Planar resonant cavity situated at the intersection of slots (Morariu, 2009)

The resonance frequency of the cavity having dimensions:

$$l = w = 0.5\text{cm} = 0.5 \cdot 10^{-2}\,\text{m}$$

according to (36), (37), (38), for E_{001} mode is f_{rez}=2.9GHz. E_{00n} resonance modes determines resonance frequencies (n > 1) in the antenna $f = nf_o$, widening emission/reception spectrum of the antenna.

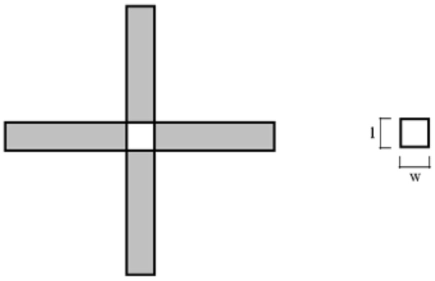

Fig. 5 Slot resonators

E_{101} mode leading to higher resonance frequencies, which in accordance with relations (36) and (37) starting with 16.7GHz.

2.2 Antenna architecture. The obtained antenna has the shape and dimensions presented in the figures 5, 6 and 7.

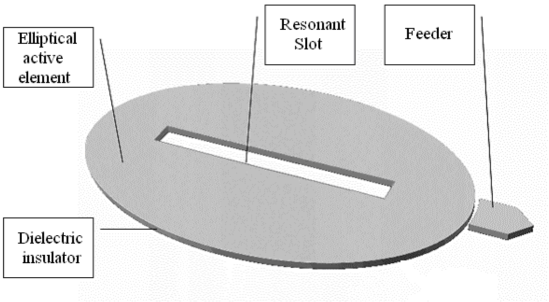

Fig. 6 Panoramic view of the stripline antenna

From physical point of view the microstrip antenna contain an active plan implemented with resonant elements in the specified frequency band, dielectrically separated by a ground conductor plan. The frontier insulation coefficient of the electromagnetic field is proportional to relative permittivity (ε_r) of the dielectric layer.

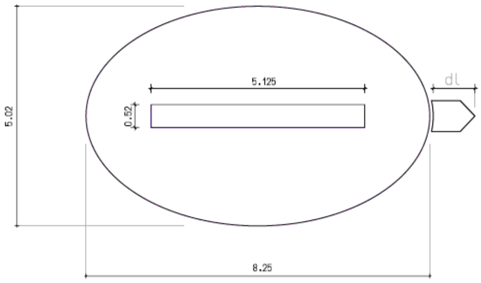

Fig. 7 Dimensions of the antenna radiant element

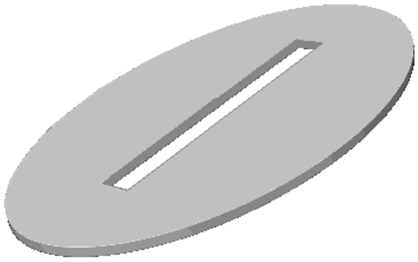

Fig. 8 Panoramic view of the radiant element

The two antenna radiating elements listed above are superimposed on the insulating layer, one on the front and the other on the back with homologous axes in angle π/2 as shown in the figure 9.

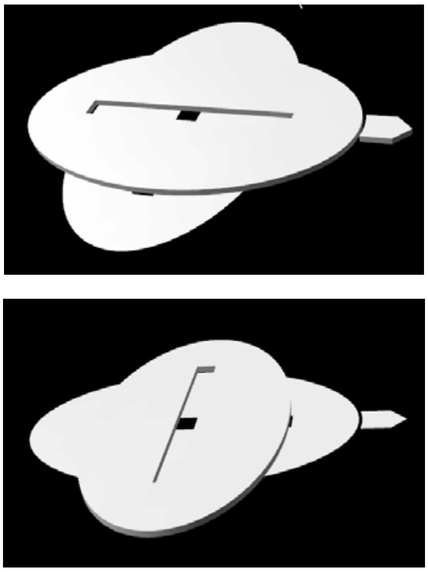

Fig. 9 Antenna front-back view

To pass the signal received or delivered, the antenna being symmetrical load, it is necessary to adapt and to make it asymmetrical for passing signal to and from the coaxial cable.

Antenna type is open dipole (figure 10) with $Z_{ant} \approx$ 40-60Ω. Value should not be adapted, but it is compulsory to make it asymmetrical (to pass to asymmetrical coaxial cable with Z = 50Ω).

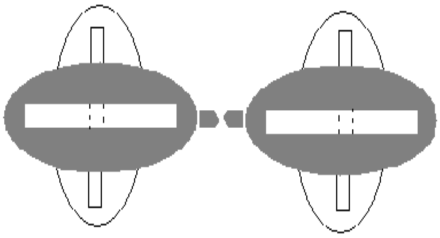

Fig. 10 Open dipole

The scheme from figure 11 has been developed to adapt to coax feeder using VSWR chart (Fig. 12). Feeder impedance adaptation is achieved by moving the point marked with (*).

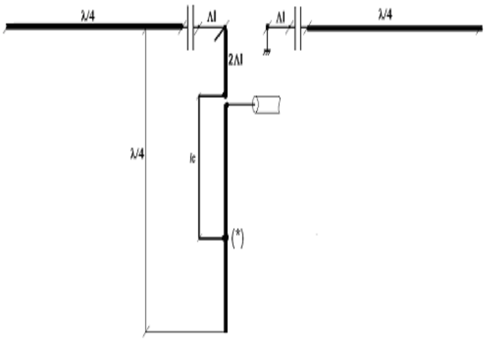

Fig. 11 Feeder matching

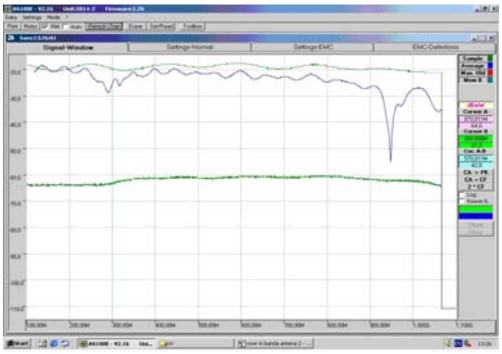

Fig. 12 VSWR in case of Γ = 1, Γ = 0 and inside band

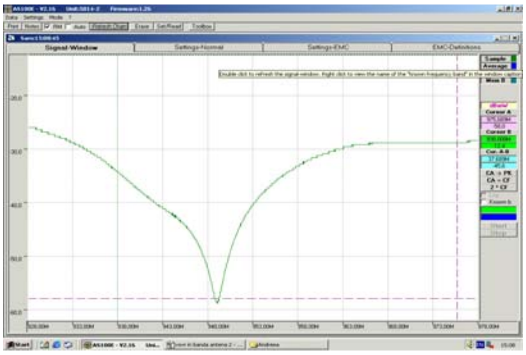

Fig. 13 50MHz opening band for VSWR 1,3,5

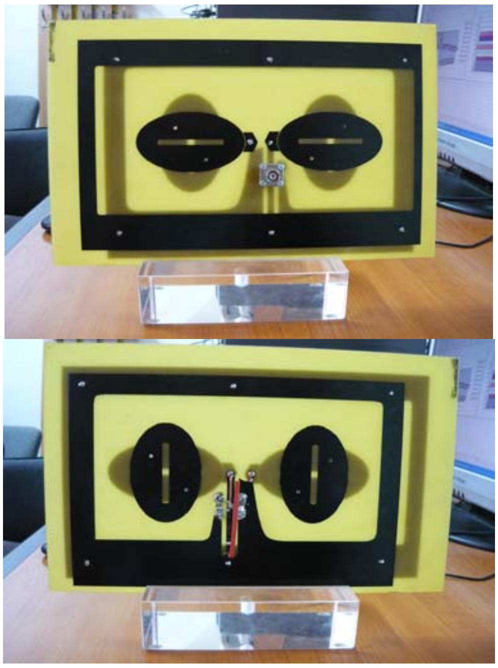

Fig. 14 Front-back view of the stripline antenna with elliptical dipoles

2.3 Experimental results. Figure 14 presents the realized stripline antenna with elliptical dipoles.

Vertically polarized stripline antenna operates from 260MHz to 1000MHz. It has two frequency bands in which operate optimally [260MHz - 470MHz and 780MHz - 1000MHz]. In case of horizontal polarization, stripline antenna operates from 230MHz to 1000MHz. Again, it operates optimally in two frequency bands [230MHz - 450MHz and 780MHz - 1000MHz].

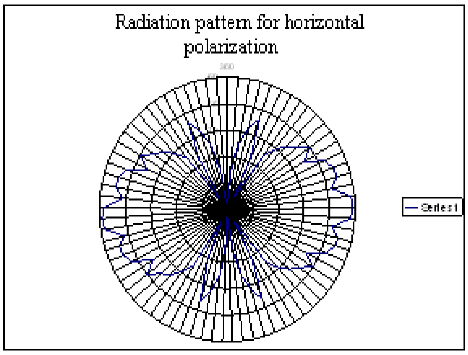

Fig. 15 Radiation pattern of the horizontally polarized stripline antenna with elliptical dipoles

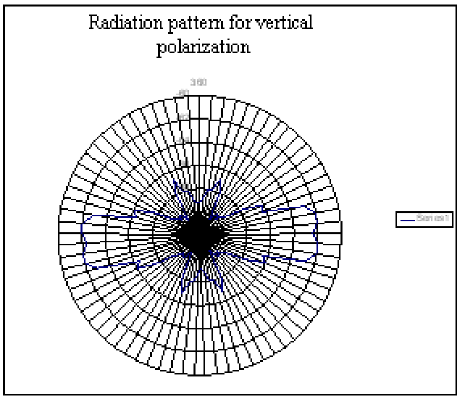

Fig. 16 Radiation pattern of the vertically polarized stripline antenna with elliptical dipoles

4. CONCLUSIONS

The design, architecture and experimentation of stripline antenna with elliptical dipoles are discussed.

The process of experimentation revealed that the proposed antenna is characterized by: important gain, wide frequency coverage band - both horizontally and vertically, very good impedance match between the antenna and feeder. Thus, adaptation to a 50ohm feeder is made with less than 0.3dB loss. Also, it appeared that the feeder matching is possible in a relatively wide range (dynamic adaptation).

On the other hand, the antenna radiation pattern shows a lobe large enough in case of horizontal polarization; in case of vertical polarization the lobe is flattened out.

BIBLIOGRAPHY

1. Amman, M. (1997). Design of Rectangular Microstrip Patch Antennas for the 2.4 GHz Band. *Applied Microwave &Wireless*, pp. 24-34.
2. Balanis, C.A. (1997). *Antenna Theory, Analysis and Design*. New York: John Wiley & Sons, 2nd edition.
3. Evangelos, S.A., *et al*. (2006). Circular and Elliptical CPW-Fed Slot and Microstrip-Fed Antennas for Ultra wideband Applications. *IEEE Antennas and Wireless Propagation Letters*, Vol. 5, pp. 294-297.
4. Gueguen, E., Thudor, F., Chambelin, P.A. (2005). Low Cost UWB Printed Dipole Antenna with High Performances. *IEEE Int. Conf. UWB*, pp. 89-92.
5. Liang, G., Liu, Y., Mei, K.K. (1989). Full-wave analysis of coplanar waveguide and slotline using the time domain finite-difference method. *IEEE Transactions on Microwave Theory and Techniques*, Vol. 17, pp. 1949-1957.
6. Marchais, C., Le Ray, G., Sharaiha, A. (2006). Stripline slot antenna for UWB communication. *IEEE Antennas and Wireless Propagation Letters*, Vol. 5, pp. 319-322.
7. Morariu, Ghe., Alexandru, M., Miron, M., Romanca, M., Machedon-Pisu, M., Dobrescu, A. (2009). Experiment-supported study on the bipolar disk microstrip antenna. DAAAM International Vienna – Austria: *EU Annals of DAAAM & Proceedings*.
8. Pozar, D.M., Schaubert, D.H. (1995). *Microstrip Antenna,* Piscatayway: IEEE Press.
9. Stutzman, W.L., Thiele, G.A. (1998). *Antenna Theory and design*, 2nd Ed. New York: John Wiley & Sons.
10. Wong, K.L. (1999). *Design of Nonplanar Microstrip Antennas and Transmission Lines*. New York: John Wiley & Sons.